

Subregional Anatomical Distribution of T2 Values of Articular Cartilage in Asymptomatic Hips

Cartilage
2014, Vol. 5(3) 154–164
© The Author(s) 2014
Reprints and permissions:
sagepub.com/journalsPermissions.nav
DOI: 10.1177/1947603514529587
cart.sagepub.com



Charles P. Ho¹, Rachel K. Surowiec¹, Fernando P. Ferro¹, Erin P. Lucas¹,
Adriana J. Saroki¹, Grant J. Dornan¹, Eric K. Fitzcharles¹, Adam W. Anz²,
W. Sean Smith¹, Katharine J. Wilson¹, and Marc J. Philippon²

Abstract

Objective: A standardized definition of normative T2 values across the articular surface of the hip must be defined in order to fully understand T2 values for detecting early degeneration. Therefore, in this article, we seek to lay foundational methodology for reproducible quantitative evaluation of hip cartilage damage using T2 mapping to determine the normative T2 values in asymptomatic individuals. **Design:** Nineteen prospectively enrolled asymptomatic volunteers (age 18–35 years, males 10, females 9, alpha angle $49.3^\circ \pm 7.2^\circ$) were evaluated with a sagittal T2 mapping sequence at 3.0 T magnetic resonance imaging. Acetabular and femoral cartilage was manually segmented directly on the second echo of the T2 mapping sequence by 3 raters, twice. Segmentations were divided into 12 subregions modified from the geographic zone method. Median T2 values within each subregion were compiled for further analysis and interrater and intrarater reliability was assessed. **Results:** In the femur, the posterior-superior subregion was significantly higher ($P \leq 0.05$) than those in the posterior-inferior and anterior-inferior subregions. In the acetabulum, the anterior-inferior subregion was significantly higher ($P \leq 0.001$) than in the anterior-superior, middle, and posterior-inferior subregions. T2 values of the posterior-superior subregion were significantly higher ($P \leq 0.05$) than the anterior-superior, middle, and posterior-inferior subregions. Interrater agreement was generally fair to good.

Keywords

articular cartilage, tissue, magnetic resonance imaging, diagnostics, hip, joint involved

Introduction

The lack of sensitivity offered by conventional magnetic resonance imaging (MRI) makes the assessment of an individual's cartilage health status challenging, especially at the earliest stages of degeneration when intervention may be the most beneficial.¹ This lack of sensitivity, specifically in the hip, can be attributed to many factors, including the inherently thin cartilage of the hip joint, the spherical joint anatomy, which lends itself the partial volume averaging, and can be susceptible to the magic angle effect. Quantitative biochemical MRI techniques, in particular T2 mapping, are being investigated as a useful addition to conventional MRI images for evaluating cartilage health.

T2 mapping is able to quantitatively evaluate articular cartilage through its sensitivity to water content and collagen anisotropy. The quantitative nature of this technology can serve as an attractive biomarker for osteoarthritis (OA) because the technique is noninvasive, commercially available, and has a relatively shorter acquisition time compared with other biochemical MRI techniques.^{1,2} By evaluating

the biochemical properties that specifically indicate cartilage health, T2 mapping may allow for earlier cartilage damage detection and potentially prove useful in longitudinal monitoring of the disease.³ Recognition of OA at an early stage through T2 mapping provides the opportunity to delay the onset of the disease by clinical and/or surgical intervention, as well as provide valuable knowledge of the grade and location of cartilage damage to aid in pre-surgical planning.^{2,4} Supporting this potential, other studies have recently investigated the role of biochemical MRI in the assessment of hip pathologies that are well known for causing premature OA, such as hip dysplasia and slipped capital femoral epiphysis.^{5,6}

¹Steadman Philippon Research Institute, Vail, CO, USA

²The Steadman Clinic, Vail, CO, USA

Corresponding Author:

Charles P. Ho, Steadman Philippon Research Institute, 181 W. Meadow Drive, Suite 1000, Vail, CO 81657, USA.

Email: charles.ho@sprivaill.org

Before T2 mapping can be used to evaluate cartilage in the clinical setting, a quantitative definition of normative, asymptomatic T2 values should be defined for each joint using a standardized and reproducible methodology. Hip joint cartilage topography analysis with T2 mapping has been performed by Watanabe *et al.*,⁷ who observed topographic variations in T2 values in healthy volunteers with no differences observed in T2 values between right and left or between male and female. However, only a single mid-head slice acquisition of T2 values was analyzed, and this study did not provide measurements for the entire chondral surface of the femur or the acetabulum. The literature currently lacks methodology for analyzing the entire hip joint by dividing it into clinically relevant hip subregions reporting quantitative MRI values that can be replicated longitudinally and across medical centers.

Using a standardized methodology to understand cartilage degeneration in the hip is currently of particular interest because of femoroacetabular impingement (FAI).⁸ Considered a contributor to OA, FAI occurs when either the femoral neck or acetabular rim have abnormal morphology that causes impingement. Therefore, in this article, we seek to lay foundational methodology for reproducible quantitative evaluation of hip cartilage damage using T2 mapping to determine the normative T2 values in asymptomatic individuals. We hypothesize that the biomechanics of the hip joint naturally create variations in cartilage degeneration in the asymptomatic population, free of symptoms and OA as assessed by physical examination and conventional MRI, which correlates with differences in T2 parameters between the various geographic zones/subregions.

Methods

This study was approved by our institutional review board and all volunteers provided informed consent. Nineteen asymptomatic volunteers (age 18-35 years, males 10, females 9, alpha angle $49.3^\circ \pm 7.2^\circ$, body mass index $24.0 \pm 2.8 \text{ kg/m}^2$) were prospectively enrolled. Volunteers were deemed asymptomatic by a self-administered subjective scoring form, an objective clinical examination performed by a sports medicine orthopedic surgeon, and by morphological MRI examination by a musculoskeletal radiologist. The self-administered subjective scoring form was used as the first measure of the screening process for inclusion into the asymptomatic study and included the Visual Analogue Score, The Tegner Score, and a Modified Harris Hip Score. Results from the scores indicated whether the subject could move onto clinical examination and are not reported as outcomes.⁹⁻¹¹ Clinical examination included evaluation of limb alignment, pain/tenderness, and the following tests: Faber test, hip dial test, anterior impingement sign, and evaluation of range of motion in the supine (flexion, abduction, and adduction) and prone (internal and external) positions.

Exclusion criteria included symptoms (e.g. pain, stiffness, and swelling exceeding mild levels) in the hip and/or knee of the imaged side, prior injury or surgery in the hip and knee, history of inflammatory arthritis or infection within the joint of interest, and evidence of high-grade cartilage lesions (i.e., International Cartilage Repair Society [ICRS] grades 3-4) from a conventional morphological MRI examination using the Hip Osteoarthritis MRI Scoring System [HOAMS] score.^{12,14}

Image Acquisition and Morphological Analysis

Magnetic resonance imaging of the hip joint was performed supine at 3.0T (Magnetom Verio, Siemens Medical Solutions, Erlangen, Germany) using a 4-channel Large Flex Coil (Siemens Medical Solutions, Erlangen, Germany). The time delay between lying on the scanner table for the MR session and acquisition of the first sequences was limited to less than five minutes in all volunteers.

The scan protocol consisted of (1) a 3-dimensional (3D) fat-suppressed Sampling Perfection with Application optimized Contrasts using different flip angle Evolution (FS SPACE) scan; (2) a multi-echo spin echo T2 mapping scan in the sagittal plane (MESE T2 Map Sag); (3) a T2 weighted turbo-spin echo sequence in the axial plane (T2w TSE Ax); (4) a proton density turbo-spin echo scan in the coronal plane (PD TSE Cor); and (5) a limited axial T1 scan distally at the level of the knee and femoral condyles for evaluation of femoral version. The SPACE scan was reformatted in all 3 planes, including oblique axial images along the femoral neck/head axis for evaluation of alpha angle. Detailed scan parameters for all sequences are depicted in **Table 1**. The T2 mapping sequence was performed at the end of the examination following morphological scans, approximately 17 minutes after entering the scanner to allow for unloading of the cartilage in a clinical scan time slot.¹³

To investigate the presence of pathology within the joint of the asymptomatic volunteers, the HOAMS was used to grade the MR images of each individual.¹⁴ The HOAMS system is a semiquantitative MRI-based scoring system of hip osteoarthritis that grades 13 articular features, including cartilage, bright marrow lesions (BMLs), subchondral cysts, osteophytes, labrum, synovitis, effusion, loose bodies, attrition, trochanteric bursitis, insertional tendonitis of the greater trochanter, paralabral cysts, and herniation pits.¹⁴ A board-certified musculoskeletal (MSK) radiologist with 17 years of experience conducted the grading of the MR studies. For cartilage, BML, and subchondral cyst assessment, the acetabulum and femur were divided into 9 subregions for cartilage evaluation and 15 subregions for acetabular and femoral subchondral bone marrow assessment as described in detail by Roemer *et al.*¹⁴ In our study, a distinction (where possible) was made between the acetabular and femoral cartilage, which was not made in the

Table 1. Parameters of the Imaging Sequences Used in the Study.

Sequence	T2 map sag	PD-TSE SPACE sag	T2w-TSE ax	T2w-PD-TSE cor	T1-TSE ax
Repetition time (ms)	2,080	1,500	3,990	3,130	700
Echo time (ms)	18.0, 36.0, 54.0, 72.0, 90.0	44	91	30	33
Field of view (mm)	200	192	165	175	280
Matrix	256 × 256	256 × 256	256 × 192	320 × 256	256 × 192
Voxel size (mm)	0.8 × 0.8 × 2.0	0.8 × 0.8 × 0.9	0.9 × 0.6 × 3.0	0.9 × 0.7 × 3.0	1.6 × 1.1 × 5.0
Slice thickness (mm)	2	0.9	3	3	5
Distance factor (%)	100	—	10	10	10
Number of slices	20	96	38	30	15
Echo trains/slice	—	—	6	24	9
Turbo factor	—	84	20	8	20
Examination time	6:45	8:00	1:45	2:35	0:37

Magnetic resonance parameters for quantitative and morphological imaging: Sag = sagittal; map = mapping; PD = proton density; TSE = turbo spin echo; SPACE = single slab 3-dimensional TSE sequence (Sampling Perfection with Application optimized Contrasts using different flip angle Evolution); Ax = axial; Cor = coronal.

HOAMS scoring system. Cartilage, BMLs, subchondral cysts, osteophytes, labral lesions, effusion, and loose bodies were graded on a numeric scale with the lower number being either no pathology or the least amount identifiable.¹⁴ Attrition, dysplasia, trochanteric bursitis, insertional tendonitis, and herniation pits were graded as present or absent.¹⁴ All our studies were nonenhanced and synovitis is not graded on nonenhanced studies.

The alpha angle was determined for a more thorough evaluation of this asymptomatic population. The alpha angles for each volunteer were obtained from an oblique axial reformation of the SPACE scan using the measurement technique described by Nötzli et al.¹⁵ We used an oblique axial slice parallel to the axis of the femoral neck and closest to the center of the femoral head. From the femoral head center, the point “hc” was defined and a perfect circle was drawn around that point which encompassed the cartilage-covered part of the femoral head. Point A was determined as the most anterior point at which the bone cortex exceeds the radius of the circle. A line from point “hc” to the center of the neck at its narrowest point (“nc”) defined the femoral neck axis. The alpha angle was measured laterally from the femoral neck axis to point A. The alpha angle is between the lines A-hc and hc-nc (**Fig. 1**). Using this technique, the angle is smaller if the femoral head is spherical and has a slim head-neck junction, yet larger if decreased head-neck offset and a cam lesion are present.

Image Analysis

Acetabular and femoral cartilage were manually segmented using Mimics software (Materialise, Plymouth, MI) directly on the second echo of the T2 mapping sequence on a slice-by-slice basis spanning all slices by 3 raters (1 orthopedic surgeon, 2 MSK radiologists). **Figure 2** depicts the full segmentation regions for the acetabular and femoral cartilage

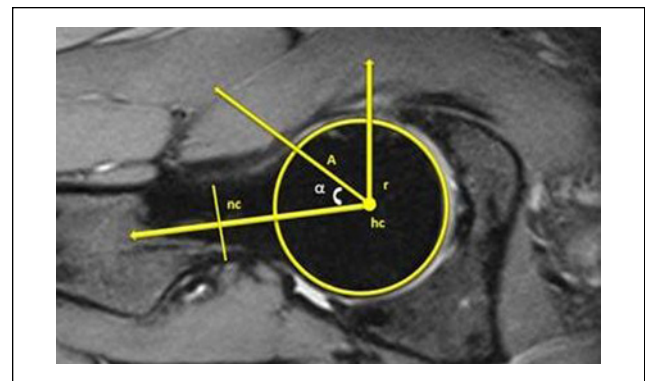


Figure 1. Magnetic resonance image depicting the alpha angle measurement. Point A is the anterior point where the distance from the center of the head (hc) exceeds the radius (r) of the subchondral surface of the femoral head. The alpha angle is measured as the angle between A-hc and hc-nc, where “nc” is the center of the neck at the narrowest point.

prior to subregion division. Segmentations were performed twice, with 30 days observed between segmentations, in order to evaluate inter- and intrarater reliability of the segmentations. To facilitate the exclusion of areas of synovial fluid and chemical shift artifact, the raters simultaneously examined the corresponding sagittal fat suppressed SPACE sequence on a neighboring monitor.

The geographic zone method described by Ilizaliturri et al.¹⁶ is used and adopted in this study to analyze T2 values in subregions created using bony landmarks. The geographic zone method divides the cartilage into 6 subregions each for the acetabulum and femur. This method is being used more frequently by the orthopedic community since its original description and may translate well to quantitative image analysis. Using 2D multislice acquisition with relatively thin slice thickness and 3D bone models of the acetabulum and femur, data collection and analysis can be

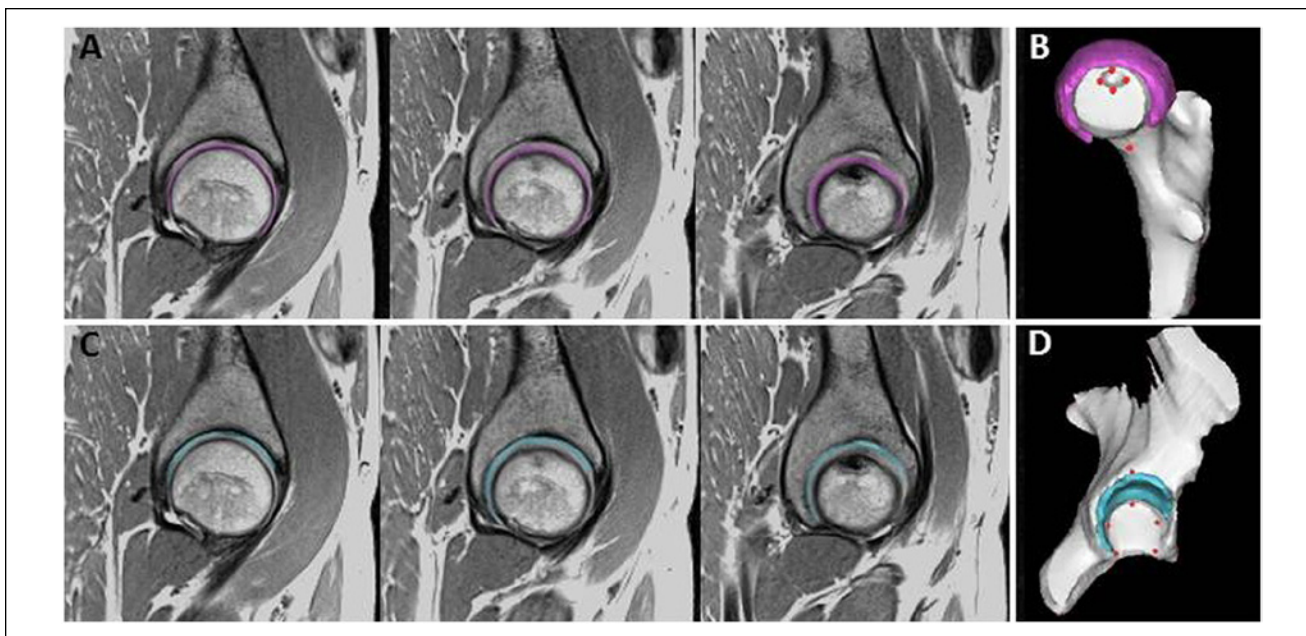


Figure 2. Depiction of segmentation on the second echo of the sagittal T2 mapping sequence in one asymptomatic subject by one rater. **(A)** Femoral cartilage segmentation on 3 consecutive slices (lateral to medial). **(B)** Three-dimensional reconstruction/visualization of cartilage segmentation overlaid on the bone model. **(C)** Acetabular cartilage segmentation on three consecutive slices. **(D)** Three-dimensional reconstruction/visualization of entire cartilage segmentation overlaid on the bone model. Red circles in **(B)** and **(D)** represent landmarks manually chosen by the raters.

Note: three consecutive slices are shown; however, raters segmented all slices.

accurately replicated and standardized. For division into the 12 subregions (6 femoral and 6 acetabular) adopted from the geographic zone method, a set of 14 bone landmarks, visible on both MRI and during arthroscopy, were developed in order to aid in reproducibly dividing the cartilage.^{16,17} The method for dividing the subregions using the landmarks is described in detail in our previous work.¹⁷ Each rater manually selected bone landmarks in Mimics by placing the landmark directly on the subject's specific bone model. The subject specific 3D bone models were created by segmenting the bone contours of the T2 mapping sequence based on the low/absent signal of the subchondral cortical bone surface and, using the segmentations, the subject's 3D bone geometries of the acetabulum and femur were reconstructed in Mimics. Using a split screen view, the 3D bone models that triangulated to the second echo of the T2 image, which allowed the rater to adjust landmark placement based on the MRI. The 14 anatomical bone landmarks are described in **Table 2** and depicted on both the 3D bone models and on the T2 mapping sequence in **Figure 3**. The coordinates (x , y , z) of these landmarks were exported and were used in a custom Matlab program (Mathworks, Natick, MA) for cartilage division into the 12 subregions.

T2 values were calculated using a Siemens WIP (work in progress) algorithm, modified from the Siemens MapIt software algorithm (Siemens Medical Solutions, Erlangen, Germany). The cartilage segmentations (femoral and

acetabular) were exported from Mimics as binary images and imported into the custom Matlab program along with the coordinates of the landmarks and the corresponding T2 maps. The program automatically divided the segmentation masks with the T2 overlay into the proposed 12 subregions using the 3D coordinates of the 14 bone landmarks. T2 parameters (mean, median, minimum, maximum, and number of pixels) for each subregion were then determined. Only T2 values between 10.0 and 110.0 ms were included in analysis in order to exclude outliers such as subchondral bone and synovial fluid (T2 values > 110.0 ms), and T2 values rejected due to poor fit (T2 values of 0.0 ms).

Statistical Analysis

Median T2 values within each subregion were compiled for further analysis. The median T2 value was chosen to summarize the T2 measurements in each subregion for each subject to reduce skewing by possible outlying values from segmentation margins and partial volume artifact. All subsequent comparison testing between subregions used the mean of these median values of all the subjects as data. To assess the repeatability of the segmentations, single measure intraclass correlation coefficients (ICCs) of median T2 values in each subregion were calculated via a 2-way random-effects model. This method

Table 2. Description of Anatomical Location of the Landmarks of the Femur and Acetabulum.

	Landmark	Description of Anatomical Location
Femur	Femoral fovea (sup/inf)	The most superior and inferior portion of the femoral fovea
	Femoral fovea (med/lat)	The most medial and lateral portion of the femoral fovea
	Head and neck junction (sup/inf)	The most superior and inferior portion of the head and neck junction of the femur
	Head and neck junction (med/lat)	The most medial and lateral portion of the head and neck junction of the femur
Acetabulum	Acetabular fossa (ant/post)	The most anterior and posterior portion of the acetabular fossa where there is no cartilage articulation
	Acetabular fossa (sup)	The most superior portion of the acetabular fossa where there is no cartilage articulation
	Insertion transverse ligament (ant/post)	The anterior and posterior insertions of the transverse ligament at the most inferior portion of the acetabular fossa
	Acetabular rim (superolateral)	Placed halfway between the ant/post transverse ligament landmarks by finding midpoint and creating an orthogonal line to the midpoint of the superolateral aspect of the acetabular rim

Med = medial; lat = lateral; inf = inferior; sup = superior; post = posterior; ant = anterior.

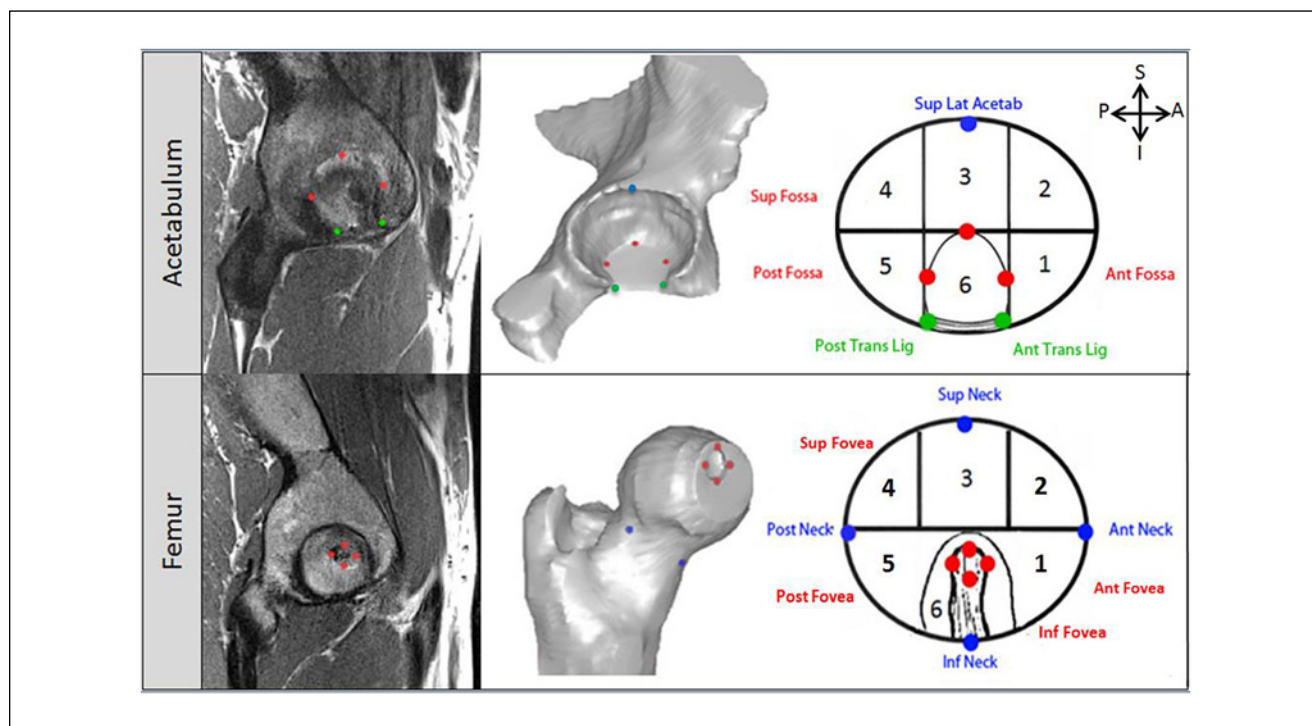


Figure 3. Adapted geographic zone method mapping system (Ilizaliturri *et al.*¹⁶) and bone landmarks. Subregions within the acetabular and femoral cartilage were divided based on the set of bone landmarks (red, blue, and green circles) on the magnetic resonance image (far left) and bone model (center) were manually identified on every volunteer by the 3 raters.

allows for generalization to a single future rater. Interpretation of ICCs was guided by Fleiss¹⁸: 0.75 to 1.00 = excellent reliability, 0.40 to 0.75 = fair to good reliability, 0.00-0.40 = poor reliability. Pearson correlations were used to check for association between alpha angle and T2 values.

Repeated-measures fixed-effects models were used to compare means (of median T2 values) between

subregions. Analysis of model residuals was performed to check whether the parametric assumptions of normality, homogeneity of variance and independence of errors were met. All pairwise comparisons of subregions were made in the femur and acetabulum separately and Bonferroni corrections were applied. All statistical analyses were performed using SPSS Version 20 (IBM Corporation, Armonk, NY).

Table 3. Results From the Semiquantitative Hip Osteoarthritis Magnetic Resonance Imaging (MRI) Scoring System (HOAMS) to Investigate Any Present Pathology Using Conventional MRI.

Subject	Category											
	Cartilage	Bone Marrow Lesion	Subchondral Cyst	Osteophyte	Labrum	Loose Bodies	Dysplasia	Trochanteric Bursitis	Insertional Tendonitis	Herniation Pits	Joint Effusion	Attrition
1	0	0	0	0	2	0	Absent	Absent	Absent	Absent	0	Absent
2	0	2	0	0	2	0	Absent	Absent	Absent	Absent	0	Absent
3	0	0	0	2	1	0	Absent	Absent	Absent	Present	0	Absent
4	0	0	0	0	2	0	Absent	Absent	Absent	Absent	0	Absent
5	0	0	0	0	1	0	Absent	Absent	Absent	Absent	0	Absent
6	0	0	0	0	2	0	Absent	Absent	Absent	Absent	1	Absent
7	0	0	0	0	1	0	Absent	Absent	Absent	Absent	0	Absent
8	0	1	0	0	2	0	Absent	Absent	Absent	Absent	0	Absent
9	0	0	0	1	1	0	Absent	Absent	Absent	Absent	1	Absent
10	0	0	0	1	2	0	Absent	Absent	Absent	Absent	1	Absent
11	0	0	0	0	1	0	Absent	Absent	Absent	Absent	0	Absent
12	0	0	0	0	1	0	Absent	Absent	Present*	Absent	0	Absent
13	0	0	0	0	1	0	Absent	Absent	Absent	Absent	1	Absent
14	1	0	1	0	2	0	Absent	Absent	Absent	Absent	1	Absent
15	0	0	1	0	2	0	Absent	Absent	Absent	Absent	0	Absent
16	2	0	0	0	2	0	Absent	Absent	Absent	Absent	0	Absent
17	0	0	0	0	1	0	Absent	Absent	Present*	Absent	0	Absent
18	0	0	0	0	2	0	Absent	Absent	Absent	Absent	0	Absent
19	2	0	0	0	2	0	Absent	Absent	Absent	Absent	0	Absent

*Denotes "very mild."

Table 4. Interrater and Intrarater Intraclass Correlation Coefficients (ICCs).

Subregion Name	Zone	Interrater Reliability			Intrarater ICCs			
		ICC	Lower	Upper	Rater 1	Rater 2	Rater 3	
Femur	Inferior-anterior	Zone 1	0.65	0.40	0.84	0.86	0.74	0.77
	Superior-anterior	Zone 2	0.68	0.46	0.85	0.80	0.88	0.93
	Superior-middle	Zone 3	0.24	-0.04	0.55	0.51	0.70	0.80
	Superior-posterior	Zone 4	0.66	0.42	0.84	0.73	0.73	0.66
	Inferior-posterior	Zone 5	0.34	-0.03	0.71	0.45	0.67	0.70
Acetabulum	Inferior-anterior	Zone 1	0.56	0.02	0.96	0.65	0.88	0.82
	Superior-anterior	Zone 2	0.54	0.21	0.78	0.83	0.80	0.91
	Superior-middle	Zone 3	0.60	0.33	0.80	0.61	0.53	0.84
	Superior-posterior	Zone 4	0.57	0.30	0.79	0.68	0.76	0.68
	Inferior-posterior	Zone 5	0.37	0.04	0.71	0.76	0.20	0.76

The inferior-middle subregion, Zone 6, was omitted from analysis. ICC = intraclass correlation coefficient; lower and upper refer to the bounds of the 95% confidence interval.

Results

Magnetic Resonance Imaging Scoring

The results from the HOAMS score are depicted in **Table 3**. No volunteer was excluded based on the HOAMS scores. All the HOAMS scores were in the lower range.

Rater Reliability

Inter- and intrarater ICCs are reported in **Table 4**. Interrater agreement was generally fair to good except in the middle-superior and posterior-inferior aspects of the femur and the posterior-inferior aspect of the acetabulum where agreement was poor. Intra-rater agreement for rater 3 was good to excellent in all subregions.

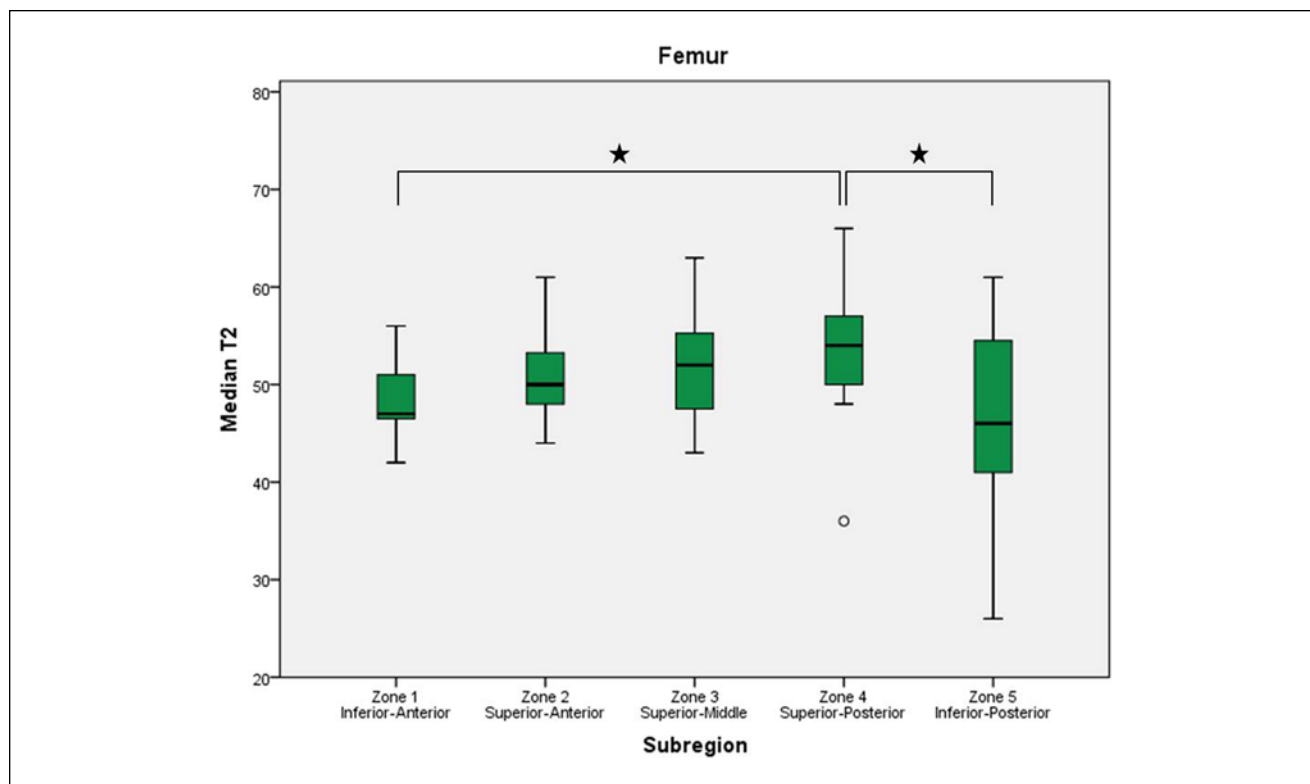


Figure 4. Boxplots display the first, second (median), and third quartiles of the T2 values in each femoral zone. Whiskers represent the minimum and maximum T2 measurements except when a circle indicates an observed value more than 1.5 times the interquartile range away from the box. Asterisks indicate significant difference between subregions.

Alpha Angles

Mean (SD) alpha angle among the subjects was 49.3° (7.2°), and the 3 largest alpha angles were 54° , 61° , and 71° . Alpha angle was significantly correlated with T2 values neither in the acetabulum ($r = 0.104$, $P = 0.671$) nor in the femur ($r = 0.195$, $P = 0.425$).

T2 Values

Quantifying and Comparing T2 Values between Subregions. **Figures 4** of femur and **5** of acetabulum display mean (\pm SD) of median T2 values for the subregions. .

Femur. Summary statistics, including 95% confidence intervals, for the means for the T2 values in the 5 subregions of the femur are included in **Table 5**. Means ranged from 46.9 to 53.9 ms. The posterior-superior aspect exhibited the highest T2 values and was significantly higher than those in the posterior-inferior aspect ($P = 0.011$) and anterior-inferior aspect ($P = 0.049$).

Acetabulum. Summary statistics, including 95% confidence intervals, for the T2 values in the 5 subregions of the

acetabulum are included in **Table 5**. Means ranged from 45.3 to 52.6 ms. The anterior-inferior portion exhibited the highest T2 values and was significantly higher than those in the anterior-superior ($P < 0.001$), middle ($P < 0.001$), and posterior-inferior ($P = 0.001$) subregions. The posterior-superior aspect also exhibited a mean T2 value that was significantly higher than the anterior-superior ($P = 0.009$), middle ($P = 0.001$), and posterior-inferior ($P = 0.023$) subregions.

Discussion

The accurate noninvasive diagnosis of cartilage degeneration in the hip before radiographical signs of OA remains challenging. The possibility of assessing the hip cartilage with morphological and biochemical MRI in asymptomatic patients has been gaining interest in the orthopedic community.^{19,20} Our study describes a set of clinically relevant subregions, adopted from the geographic zone method, to describe T2 values in both the acetabular and femoral cartilage in the asymptomatic hip. The most important finding of the present study was that significant differences in median T2 values were observed among the different

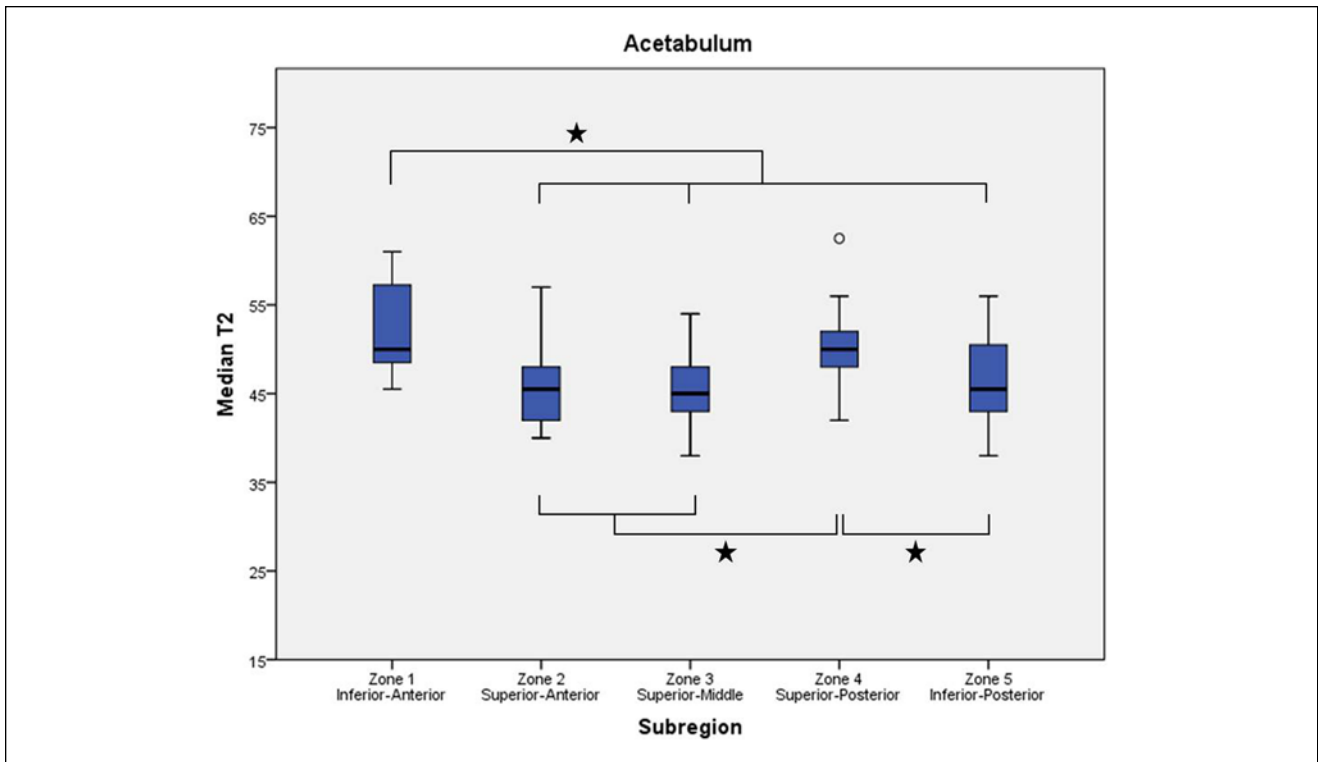


Figure 5. Boxplots display the first, second (median), and third quartiles of the T2 values in each acetabular zone. Whiskers represent the minimum and maximum T2 measurements except when a circle indicates an observed value more than 1.5 times the interquartile range away from the box. Asterisks indicate significant difference between subregions.

Table 5. Summary Statistics, Including 95% Confidence Intervals, of the Means for the T2 Values in the 5 Subregions of the Acetabulum and Femur.

Summary of T2 Values						95% Confidence Interval of the Mean			
	Zone	N	Mean	Standard Deviation	Minimum	Maximum	Lower	Upper	
Femur	Inferior-anterior	Zone 1	19	48.5	3.7	42	56	46.7	50.3
	Superior-Anterior	Zone 2	19	51.1	4.5	44	61	49.0	53.3
	Superior-middle	Zone 3	19	51.9	5.5	43	63	49.2	54.5
	Superior-posterior	Zone 4	19	53.9	6.5	36	66	50.8	57.1
	Inferior-posterior	Zone 5	14	46.9	10.1	26	61	41.1	52.8
Acetabulum	Inferior-anterior	Zone 1	7	52.6	5.9	45.5	61	47.1	58.0
	Superior-anterior	Zone 2	19	46.0	4.7	40	57	43.8	48.3
	Superior-middle	Zone 3	19	45.3	4.2	38	54	43.3	47.4
	Superior-posterior	Zone 4	19	50.1	4.5	42	62.5	47.9	52.2
	Inferior-posterior	Zone 5	14	46.1	5.3	38	56	43.0	49.1

The inferior-middle subregion, Zone 6, was omitted from analysis.

subregions, corroborating our hypothesis by demonstrating that the biomechanics of the hip joint naturally create variations in cartilage T2 values, even in the asymptomatic population. This means that there is not one single “normal” T2 value for asymptomatic cartilage within the hip

joint and that the location of the natural variation of T2 values therefore becomes important. With the proposed methodology, inter-rater agreement proved to be generally fair to good. An exception was observed in the middle-superior and posterior-inferior aspects of the femur

(femoral zones 3 and 5) and the posterior-inferior aspect of the acetabulum (zone 5) where agreement was deemed poor. Even so, intrarater agreement for rater 3 (MSK-trained radiologist) was good to excellent in all subregions.

In an attempt to ensure that our asymptomatic cohort had a “normal” proximal femur morphology, we measured the alpha angles of all volunteers. We observed an average alpha angle of 49°, which is considered normal according to the literature.^{21,22} Interestingly, recent research has shown that biochemical MRI may detect early chondral damage in asymptomatic subjects with abnormally high alpha angles, and that the severity of the damage correlates with cam deformity severity.⁸ On the other hand, our study was done on subjects *without* cam deformity, and we did not observe a similar correlation between increasing T2 values and increasing alpha angles. These findings suggest that the alpha angle can be a predictor of chondral damage for subjects *with* cam deformity, but that does not necessarily apply for the overall population *without* a cam.

We observed that the load bearing portion of the femoral head (superior-anterior, middle, and superior-posterior) have T2 values that are higher than the non-weightbearing portions (inferior-anterior and inferior-posterior). This variation had been anticipated, since portions of the femoral head that are not exposed to weight-bearing are expected to have a different collagen and water content. We also expected the superior-anterior zone (zone 2) to have higher values than the superior-posterior (zone 4). Because of normal hip biomechanics, the flexion movement should cause greater stress in the anterior cartilage. However, our findings did not corroborate this. Yet in the flexed position it was hypothesized that the femoral axis force may be greater in the posterior superior zone (zone 4). We postulate that we were unable to observe a significant difference because the zone system we used includes large medial to lateral portions of the articular surface, which may “wash out” minor differences and does not account for medial/lateral variations. Another possibility is that such a difference is not big enough to be observed in an asymptomatic cohort. In FAI patients, a significant difference could be reached when comparing the anterior and posterior zones of the weight-bearing cartilage. Such a pattern has already been demonstrated in dGEMRIC studies, where it was observed that cam-FAI patients have cartilage lesions in the anterior-superior zone more frequently than controls.²³ The same study observed chondral damage in the posterior zone for pincer type FAI patients, confirming the “contrecoup lesion”—a specific pattern of chondral damage observed in the posterior acetabulum with pincer type FAI, secondary to a levering mechanism due to anterior impingement.²⁴

In the acetabular side, we detected similar T2 values for the superior-anterior and middle zones (zones 2 and 3), with slightly increased values for the superior-posterior zone

(zone 4). This finding is in accordance with a previous study that employed dGEMRIC to compare different zones of the hip joint.²⁵ We theorize that this pattern could be reversed in subjects with FAI, due to the chondral damage that is observed in the anterior-superior portion of the acetabular cartilage, particularly in the most lateral portion.²⁵

In a recent study, dGEMRIC findings were analyzed in subjects with normal femoral morphology and asymptomatic subjects with cam deformity.^{8,23} The authors of the study concluded that cam deformity is associated with cartilage damage, even before the onset of symptoms. This study highlights the potential for an earlier diagnosis using biochemical MRI. However, dGEMRIC requires the use of a contrast agent and has an inherently long acquisition time, limiting its widespread clinical application. Additionally, dGEMRIC may be operator/site and technique dependent, including contrast dose and the delay time and extent of exercise between contrast administration and imaging, which hinders reproducibility and portability among centers.

Using T2 mapping, Watanabe *et al.*⁷ investigated topographic variation of hip articular cartilage in healthy volunteers. The authors concluded that topographic variations exist, and therefore should be taken into account when evaluating T2 mapping findings. However, this study evaluated a small cohort of 12 subjects and only performed their T2 evaluation at a central slice of the femoral head. Therefore, it did not provide information regarding the entirety of the hip joint cartilage surface. We present our results according to subregions adopted from hip arthroscopy literature, thus evaluating the entire chondral surface.

The posterior-superior subregion of both the acetabulum and femur had significantly higher T2 values than the posterior-inferior subregion, which is consistent with the literature. Miese *et al.*⁶ performed a similar study, looking at patients with sequelae from slipped capital femoral epiphysis. They identified significant differences between the slipped capital femoral epiphysis group and the healthy controls. Moreover, they compared different portions of the hip and concluded that the contrast was most evident in the superolateral portion of the hip joint, where the abnormal shape of the femoral head causes an abnormal force concentration that overloads the cartilage. Similarly, while investigating patients with hip dysplasia, Nishii *et al.*⁵ reached comparable conclusions.⁵ It must be emphasized that these studies also based their findings in specific ROI's that were manually defined, without a standardized routine to assess the entire hip joint. In a laboratory study, Sparks *et al.*²⁶ evaluated the load transmission between the femoral head and acetabulum, at several different positions. The authors observed that load tends to be concentrated in the superior-anterior portion of the joint in most positions, except for increased femoral adduction. This is not corroborated by our study, since we did not observe signs of load concentration in the anterior portion of the joint. We hypothesize that, in asymptomatic patients, the fluid seal effect

provided by the intact labrum is capable of distributing forces more evenly throughout the joint surface.²⁷ In a patient with FAI, it is possible that the loss of the fluid seal effect due to labral damage will alter the force transmission patterns, allowing for load concentration in the anterior-superior joint. Further studies comparing T2 mapping of all different zones in both asymptomatic and FAI groups would be fundamental to test this hypothesis.

We also observed increased T2 values in the anterior-inferior acetabular zone (zone 1), associated with a high standard deviation and lower interobserver agreement. The clinical significance of this is unclear, since this zone corresponds to the medial and inferior portion of the joint, close to the transverse ligament, where there is minimal weightbearing and chondral damage is uncommon.²⁴ We hypothesize that this occurred because of the decreased cartilage thickness in this specific zone, which may be subject to greater partial volume averaging error and compromise the precision of the manual segmentation (also demonstrated in the low interobserver ICC values). Previous studies in the knee joint also observed greater variability when cartilage thickness is reduced.²⁸

This work outlines existing differences in clinically relevant subregions of articular cartilage in terms of biochemical composition, structure and content at the asymptomatic hip joint, indicating that all subregions within the hip are unique in their make-up. It should be noted if that these observed differences of normal variation may be attributed to subregions that are affected earlier or more commonly by degeneration. Our cohort, however, was chosen to reduce this potential bias as we enrolled only young individuals (age 18-35 years) since asymptomatic degeneration is rather uncommon in this population. Previous research as demonstrated that asymptomatic individuals younger than 35 years are 13.7 times less likely to have asymptomatic chondral defects.¹⁹ Further studies are warranted to evaluate symptomatic populations and implications from interventions in the biochemical composition of the hip cartilage.

There are limitations to the present study. Evaluation of cartilage in the hip joint may be limited by utilizing segmentations from the sagittal view alone. Visualization of the most inferior aspects (zones 1 and 5) for both the femoral and acetabular cartilage may be affected by their inherently limited visualization in the sagittal plane and thus more susceptible to imaging artifact and partial volume averaging. The inferior aspects, especially the posterior inferior aspects of the femur and acetabulum (zones 5), are not common areas for the development of OA, which was echoed in the present study as the superior posterior region (zone 4) was significantly higher than the posterior inferior region (zone 5) in both the acetabulum and femur. The lack of visualization of these zones, however, could be addressed by the integration of a quantitative mapping sequence in the coronal plane. This study used manual segmentation, which

is still most reliable and widely used for research purposes. However, manual segmentation coupled with manual landmark selection would be too time intensive for inclusion clinically. Automated cartilage segmentation has recently been the focus of research and could become available for clinical use soon. This would potentially allow for reproducible and time effective evaluation of biochemical MRI values.

Conclusion

This study demonstrated characteristic patterns of cartilage T2 mapping in articular cartilage subregions of the femur and acetabulum. The proposed subregions adopted from the geographic zone method may increase the efficacy and reproducibility of quantitative MRI and may allow the data to be transferrable across centers, and different time points, and among orthopedists and radiologists to better integrate quantitative mapping from theory to practice in the clinical workflow.

Acknowledgments

The authors would like to acknowledge Bill Brock for his time and expertise in acquiring the magnetic resonance images.

Authors' Note

All work was performed at the Steadman Philippon Research Institute. The funding source did not contribute to the study design, collection, or interpretation of the data. The funding source did supply the algorithm for calculating T2 values which was their only contribution to the data analysis.

Declaration of Conflicting Interests

The author(s) declared no potential conflicts of interest with respect to the research, authorship, and/or publication of this article.

Funding

The author(s) disclosed receipt of the following financial support for the research, authorship, and/or publication of this article: This research was funded in part by a grant from Siemens Medical Solutions, USA.

Ethical Approval

This study was approved by our institutional review board.

References

1. Palmer AJ, Brown CP, McNally EG, Price AJ, Tracey I, Jeppard P, *et al.* Non-invasive imaging of cartilage in early osteoarthritis. *Bone Joint J.* 2013;95-B(6):738-46.
2. Nishioka H, Hirose J, Nakamura E, Okamoto N, Karasugi T, Taniwaki T, *et al.* Detecting ICRS grade 1 cartilage lesions in anterior cruciate ligament injury using T1ρ and T2 mapping. *Eur J Radiol.* 2013;82(9):1499-505.

3. Jazrawi LM, Alaia MJ, Chang G, Fitzgerald EF, Recht MP. Advances in magnetic resonance imaging of articular cartilage. *J Am Acad Orthop Surg*. 2011;19(7):420-9.
4. Apprigh S, Mamisch TC, Welsch GH, Stelzeneder D, Albers C, Totzke U, *et al*. Quantitative T2 mapping of the patella at 3.0T is sensitive to early cartilage degeneration, but also to loading of the knee. *Eur J Radiol*. 2010;81(4):438-43.
5. Nishii T, Shiomi T, Tanaka H, Yamazaki Y. Loaded cartilage T2 mapping in patients with hip dysplasia. *Radiology*. 2010;256(3):955-65.
6. Miese FR, Zilkens C, Holstein A, Bittersohl B, Kropil P, Mamisch TC, *et al*. Assessment of early cartilage degeneration after slipped capital femoral epiphysis using T2 and T2* mapping. *Acta Radiol*. 2011;52(1):106-10.
7. Watanabe A, Boesch C, Siebenrock K, Obata T, Anderson SE. T2 mapping of hip articular cartilage in healthy volunteers at 3T: a study of topographic variation. *J Magn Reson Imaging*. 2007;26(1):165-71.
8. Pollard TC, McNally EG, Wilson DC, Wilson DR, Madler B, Watson M, *et al*. Localized cartilage assessment with three-dimensional dGEMRIC in asymptomatic hips with normal morphology and cam deformity. *J Bone Joint Surg Am*. 2010;92(15):2557-69.
9. Tegner Y, Lysholm J. Rating systems in the evaluation of knee ligament injuries. *Clin Orthop Relat Res*. 1985;(198):43-9.
10. Brokelman RB, Haverkamp D, van Loon C, Hol A, van Kampen A, Veth R. The validation of the visual analogue scale for patient satisfaction after total hip arthroplasty. *Eur Orthop Traumatol*. 2012;3(2):101-5.
11. Hinman RS, Dobson F, Takla A, O'Donnell J, Bennell KL. Which is the most useful patient-reported outcome in femoroacetabular impingement? Test-retest reliability of six questionnaires. *Br J Sportes Med*. 2014;48(6):458-63.
12. Brittberg M, Peterson L. Introduction of an articular cartilage classification. *ICRS Newslett*. 1998;1:5-8.
13. Apprigh S, Welsch GH, Mamisch TC, Szomolanyi P, Mayerhoefer M, Pinker K, *et al*. Detection of degenerative cartilage disease: comparison of high-resolution morphological MR and quantitative T2 mapping at 3.0 Tesla. *Osteoarthritis Cartilage*. 2010;18(9):1211-7.
14. Roemer FW, Hunter DJ, Winterstein A, Li L, Kim YJ, Cibere J, *et al*. Hip Osteoarthritis MRI Scoring System (HOAMS): reliability and associations with radiographic and clinical findings. *Osteoarthritis Cartilage*. 2011;19(8):946-62.
15. Nötzli H, Wyss T, Stoecklin CH, Schmid MR, Treiber K, Hodler J. The contour of the femoral head-neck junction as a predictor for the risk of anterior impingement. *J Bone Joint Surg Br*. 2002;84(4):556-60.
16. Ilizaliturri VM, Byrd JW, Sampson TG, Guanche CA, Philippon MJ, Kelly BT, *et al*. A geographic zone method to describe intra-articular pathology in hip arthroscopy: cadaveric study and preliminary report. *Arthroscopy*. 2008;24(5):534-9.
17. Surowiec RK, Lucas EP, Wilson KJ, Saroki AJ, Ho CP. Clinically relevant subregions of articular cartilage of the hip for analysis and reporting quantitative MR imaging: a technical note. *Cartilage*. 2014;5(1):11-5.
18. Fleiss JL. *The design and analysis of clinical experiments* (Wiley series in probability and mathematical statistics: applied probability and statistics). New York, NY: Wiley; 1986.
19. Register B, Pennock AT, Ho CP, Strickland CD, Lawand A, Philippon MJ. Prevalence of abnormal hip findings in asymptomatic participants: a prospective, blinded study. *Am J Sports Med*. 2012;40(12):2720-4.
20. Bittersohl B, Zilkens C, Kim YJ, Werlen S, Siebenrock KA, Mamisch TC, *et al*. Delayed gadolinium-enhanced magnetic resonance imaging of hip joint cartilage: pearls and pitfalls. *Orthop Rev (Pavia)*. 2011;3(2):e11.
21. Nötzli H, Wyss T. The contour of the femoral head-neck junction as a predictor for the risk of anterior impingement. *J Bone Joint Surg Br*. 2002;84(4):556-60.
22. Toogood PA, Skalak A, Cooperman DRD. Proximal femoral anatomy in the normal human population. *Clin Orthop Relat Res*. 2009;467(4):876-85.
23. Bittersohl B, Steppacher S, Haamberg T, Kim YJ, Werlen S, Beck M, *et al*. Cartilage damage in femoroacetabular impingement (FAI): preliminary results on comparison of standard diagnostic vs delayed gadolinium-enhanced magnetic resonance imaging of cartilage (dGEMRIC). *Osteoarthritis Cartilage*. 2009;17(10):1297-306.
24. Beck M, Kalhor M, Leunig M, Ganz R. Hip morphology influences the pattern of damage to the acetabular cartilage. *J Bone Joint Surg Br*. 2005;87(7):1012-8.
25. Bittersohl B, Hosalkar HS, Haamberg T, Kim YJ, Werlen S, Siebenrock KA, *et al*. Reproducibility of dGEMRIC in assessment of hip joint cartilage: a prospective study. *J Magn Reson Imaging* 2009;30(1):224-8.
26. Sparks DR, Beason DP, Etheridge BS, Alonso JE, Eberhardt AW. Contact pressures in the flexed hip joint during lateral trochanteric loading. *J Orthop Res*. 2005;23(2):359-66.
27. Ferguson SJ, Bryant JT, Ganz R, Ito K. An in vitro investigation of the acetabular labral seal in hip joint mechanics. *J Biomech*. 2003;36(2):171-8.
28. Multanen J, Rauvala E, Lammentausta E, Ojala R, Kiviranta I, Hakkinen A, *et al*. Reproducibility of imaging human knee cartilage by delayed gadolinium-enhanced MRI of cartilage (dGEMRIC) at 1.5 tesla. *Osteoarthritis Cartilage*. 2009;17(5):559-64.